ACS APPLIED MATERIALS & INTERFACES

Forum Article

www.acsami.org

Stable Cycling of a Scalable Graphene-Encapsulated Nanocomposite for Lithium–Sulfur Batteries

Guang He,[†] Connor J. Hart,[†] Xiao Liang,[†] Arnd Garsuch,[‡] and Linda F. Nazar*[,†]

[†]Department of Chemistry and the Waterloo Institute for Nanotechnology, University of Waterloo, 200 University Avenue West, Waterloo, Ontario N2L 3G1, Canada

[‡]GCN/EE - M311, BASF SE, 67056 Ludwigshafen, Germany

Supporting Information

ABSTRACT: We report the synthesis of a low-cost carbon/sulfur nanocomposite using Ketjen black (KBC) as the carbon framework, encapsulated by thin graphene sheets using a simple process that relies on binding a functionalized KBC/S nanoparticle surface with graphene oxide (GO), which is reduced *in situ*. A slight excess of GO is employed to create a second layer of graphene wrapping around the KBC/S. This g-KBC/S sulfur cathode exhibits excellent cyclability over 200 cycles where the average stabilized fade rate is only 0.026% or 1.1 mAh g^{-1} per cycle. This excellent performance is primarily attributed to the wrapped, internally porous architecture. The large pore volume, small pore diameter, and uniform nanoparticle size of the mesoporous KBC array provides an ideal frame for the fabrication of a homogeneous C/S composite, whereas the graphene/GO sheets serve as an external chemical and physical barrier that inhibits polysulfide diffusion.

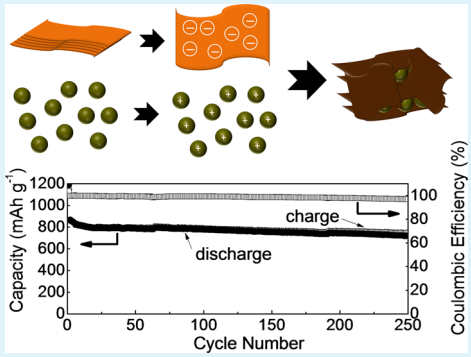

KEYWORDS: *long-life lithium sulfur battery, low-cost sulfur cathodes, graphene encapsulation*

INTRODUCTION

The Li–S battery is considered to be one of the most promising candidates for the next generation of transportation because it is safe, low-cost, and environmentally benign and exhibits much higher theoretical capacity (1675 mAh g^{-1}) and energy density (2600 Wh kg^{-1}) than the Li-ion battery.[1−4] Currently, most studies concerning Li–S batteries focus on the challenges of the sulfur cathodes: namely, suppression of the polysulfide shuttle that causes active material loss and capacity fading.[5] Many of these have involved polysulfide encapsulation based on porous carbons and graphene. Porous carbon is typically used as a framework that incorporates sulfur into its nanopores to fabricate a C/S nanostructure.[6] The pores (usually in the small meso and large micro range) restrict the soluble sulfur redox intermediates (S_n^{2-}, $4 < n < 8$) from diffusing into the electrolyte and engaging in the shuttle mechanism.[7,8] A good porous carbon sulfur host must meet the following criteria: (1) a large total pore volume to accommodate possible large sulfur content and increase the proportion of the active material in the cathode; (2) a high specific surface area for efficient contact between sulfur (or Li_2S) and carbon for efficient electron transfer; (3) an intermediate pore size that allows mass transfer but provides effective confinement of sulfur and polysulfides; and (4) a nanostructured framework that facilitates sulfur impregnation into the pores. Our group explored various ordered mesoporous carbons such as CMK-3,[9] BMC-1,[10] and spherical-BMC[11] as frameworks for Li–S cathodes and found that different pore structures lead to distinct electrochemical performance. For example, CMK-3 carbon with small mesopores (3 nm) shows very high reversible capacity (1200 mAh g^{-1}) at low/intermediate current rates (C/10 and C/5) whereas spherical-BMC nanospheres with a bimodal porous structure display high capacity (900 mAh g^{-1}) at high current rates (1C) over 100 cycles in combination with a DOL/DME electrolyte. Many other groups have also demonstrated enhanced cell performance using porous carbon frameworks.[12−16] Overall, and not surprisingly, small pores demonstrate better sulfur/polysulfide retention than large pores. Promising results have also been achieved with certain microporous carbons[12,14] assisted by carbonate electrolyte solvents. However, only one sloping plateau at ~1.8 V is observed for this type of cathode, leading to a lower energy density than for the two-plateau Li–S cells. More importantly, some groups obtained conflicting results with carbonate electrolytes,[17,18] indicating the mechanism behind the stable cycling is still not clear.

The shuttle issue can also be addressed by encapsulating the sulfur cathode particles within graphene sheets.[19] A distinct advantage for graphene-based sulfur cathodes over porous carbon cathodes is the ability to easily introduce various

Special Issue: New Materials and Approaches for Electrochemical Storage

Received: January 28, 2014
Accepted: April 2, 2014
Published: May 5, 2014

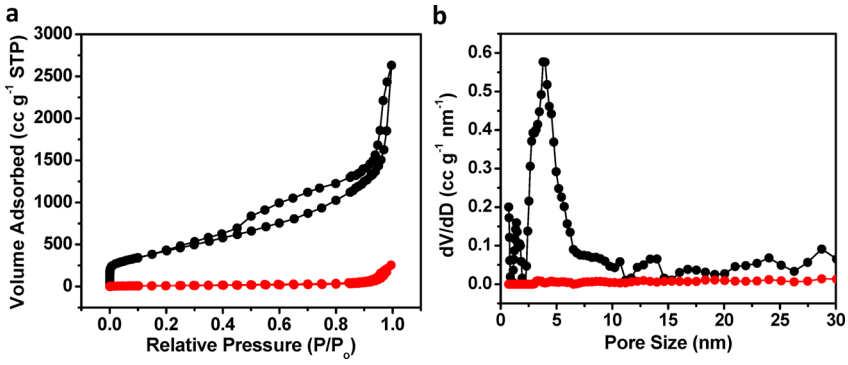

Figure 1. (a) N_2 adsorption analysis and (b) pore size distribution of KBC (black curve) and KBC/S (red curve).

functional groups on the surface. These functional groups are reported to be critical for long cycling life by benefiting the binding for polysulfides.[20,21] The most commonly used strategy to realize graphene encapsulation of sulfur particles is the reduction of graphene oxide by sodium polysulfide or sodium thiosulfate.[18,22−24] The particle size of sulfur synthesized in this way is always at the submicrometer level, 2 orders of magnitude larger than sulfur trapped in micro/mesopores. The uniform encapsulation of such large sulfur particles presents a challenge for many graphene/sulfur cathodes.[25−27] Graphene/sulfur/carbon nanotube/fiber hybrid materials[28−30] have been designed to solve this problem but the sulfur coating thickness on these 1D carbon nanoparticles is still much larger than mesopore dimensions. The development of graphene/porous carbon hybrid sulfur cathodes is another option to reduce the sulfur particle size, combining the advantages of both of these nano frameworks; nevertheless, very few studies have employed this approach so far to our knowledge.

We report here a new sulfur cathode configuration obtained by combining both porous carbons and graphene using a self-assembly process. The selected mesoporous carbon is commercially available, low cost Ketjen black (KBC), that has a large surface area and a pore volume akin to lab-made carbons. The uniform nanoscale particle size of the carbon not only facilitates sulfur incorporation into the micro/mesopores, but also provides a conductive scaffold for graphene-wrapping. Coupled with the polysulfide retention properties provided by the residual oxygen-containing functional groups on the graphene sheets, the resulting electrode exhibits high reversible capacity with exceptionally stable cycling performance. This high capacity and stable cycling implies the dual-protection provided by nanopores and graphene sheets reinforces polysulfide retention. Additionally, all the raw materials are easily obtainable and the graphene/porous-carbon/sulfur composite is prepared with a low-temperature and scalable approach, making this method very attractive for industrial adaptation.

EXPERIMENTAL PROCEDURES

Preparation of the KBC/S Nanocomposite. the KBC/S was prepared via a simple two-step strategy. First, KB carbon (Toyota) and sulfur powders were mixed (w:w = 3:7) and ball-milled for 8 h with acetone. The slurry was then dried at 60 °C and the obtained C/S was heated at 155 °C overnight to complete the impregnation of sulfur into the pores of the carbon framework.

Preparation of g-KBC/S. To fabricate g-KBC/S, the KBC/S was first functionalized by a cationic polyelectrolyte poly-(diallyldimethylammonium chloride) (polyDADMAC).[31] Specifically, 200 mg of KBC/S was dispersed in 400 mL of aqueous solution containing 0.5 wt % polyDADMAC, 20 mM NaCl, and 20 mM tris(hydroxymethyl)aminomethane. This dispersion was sonicated for 0.5 h and stirred for at least 4−6 h to introduce positively charged groups on the surface of the KBC/S. After the solid was collected by vacuum filtration and washed by DI water, 100 mg of KBC/S was redispersed in 100 mL of DI water. Separately, 20 mg graphene oxide (GO, ACS Material) was dispersed in 100 mg of DI water by sonication. The KBC/S suspension that was obtained was then slowly added into the GO dispersion and stirred for 2 h. Because of the electrostatic interaction between the positively charged KBC/S and negatively charged GO, the wrapping of KBC/S by GO sheets was achieved by self-assembly.[32] Next, 180 μL of hydrazine (35 wt %) was added into the mixture and stirred at 60 °C for 30−60 min to reduce the GO. Finally, the resulting product was filtered and dried at 60 °C overnight.

Electrode and Cell Assembly. The g-KBC/S cathode materials were slurry-cast from *N,N*-dimethylformamide onto a carbon-coated aluminum current collector, with a positive electrode formula of C/S: Super P: Kynar Flex = 80:10:10. The electrolyte was 1 M bis(trifluoromethanesulfonyl)imide lithium (LiTFSI) in a mixed solvent of 1,2-dimethoxyethane (DME) and 1,3-dioxolane (DOL) (v/v = 1:1), with 2 wt % of $LiNO_3$. The volume of electrolyte added to each cell was 50 μL per an average sulfur loading of 1.5 g cm^{-2} per electrode. Metallic lithium was used as the negative electrode.

Characterization. Surface area, pore volume and pore size were determined from nitrogen adsorption and desorption isotherms performed on a Quantachrome Autosorb-1 instrument. Before measurement the samples were degassed at either 150 °C (for KBC) or room temperature (for KBC/S) on a vacuum line. The total pore volume of carbon and the C/S composites were calculated at a relative pressure of 0.999 (P/P_o). The specific surface area and pore size distribution were determined by the Brunauer−Emmett−Teller (BET) theory and the quenched solid density functional theory (QSDFT) model from the adsorption branch of the isotherms. Field-emission scanning electron microscopy (FESEM) images were acquired on a LEO 1530 instrument. Scanning transmission electron microscopy (STEM) and high resolution transmission electron microscopy (HRTEM) were carried out on a Hitachi HD - 5200 STEM and JEOL JEM-2010, respectively. Galvanostatic cycling of the Li−S coin cells was performed on an Arbin BT-2000 at room temperature.

RESULTS AND DISCUSSION

N_2 adsorption isotherms and pore size distribution curves of both KBC and KBC/S are shown in Figure 1. The raw KBC exhibits a typical type-IV curve and capillary condensation step, indicating a mesoporous structure with narrow pore size distribution (Figure 1a, black curve). The specific BET surface area and pore volume of the KBC are 1600 m^2 g^{-1} and 4.0 cc g^{-1} (P/P_o = 0.999), respectively, much larger than many synthetic mesoporous carbons.[33,34] The pore size distribution curve reveals the large surface area and pore volume of the KBC

originates from a combination of micropores (<2 nm) and small mesopores (ca. 4.0 nm), as shown in Figure 1b (black curve, based on QSDFT model). Theoretically, as much as 80 wt % of sulfur (S:C = 4:1 in weight) could be incorporated for a carbon framework possessing a pore volume of 4.0 cc g^{-1}, based on complete conversion of sulfur (S) to lithium disulfide (Li_2S) in the cathode. However, the sudden rise of the isotherm (adsorption branch) at the region above P/P_o = 0.9 suggests that there is also meaningful contribution from the textual porosity to the total pore volume. This is due to the nanosize dimensions of the KBC, as shown in the SEM image (see Figure S1 in the Supporting Information). To estimate the intrinsic micro/meso pore volume, the cumulative volume is plotted with increasing pore diameter of the KBC nano framework (see Figure S2 in the Supporting Information), based on the QSDFT model. The result indicates the intrinsic pore volume is ca. 1.5 cc g^{-1}, comprised mostly of micropores and small mesopores with diameters less than 6 nm, which is consistent with the finding in Figure 1b. Large mesopores (6 nm < d < 15 nm) contribute approximately an additional 0.5 cc g^{-1}, for a total of ca. 2.0 cc g^{-1}. Even this significant pore volume is sufficient for 70 wt % sulfur in the C/S composite, comparable to many synthetic porous carbons prepared with elaborate methods. In addition, textural porosity (pores >15 nm that reside between the 50 nm KBC particles account for an additional ca. 2.0 cc g^{-1} pore volume. After the material is treated with sulfur, the N_2 adsorption isotherm curves (Figure 1, red curves) and the pore size distribution curve of the KBC/S composite significantly diminish. The total pore volume of KBC/S is calculated to be 0.4 cc g^{-1}, confirming the successful impregnation of sulfur into the pores.

Irrespective of internal mesoporosity, large particle-size carbon frameworks always manifest a sulfur layer on their external surface which results in an inhomogeneous sulfur distribution and difficulty for sulfur accessibility into the interior. This is solved by reducing the carbon particle size down to the nanoscale. The SEM and STEM images of the KBC/S (Figure 2a, b) show an almost identical morphology and particle size to the pristine carbon and no sulfur agglomeration between the loosely packed nanoparticles. The elemental maps of this nanocomposite also suggest a uniform distribution of sulfur into the pores of the KBC after ball-milling and heat treatment at 155 °C (Figure 2c, d).

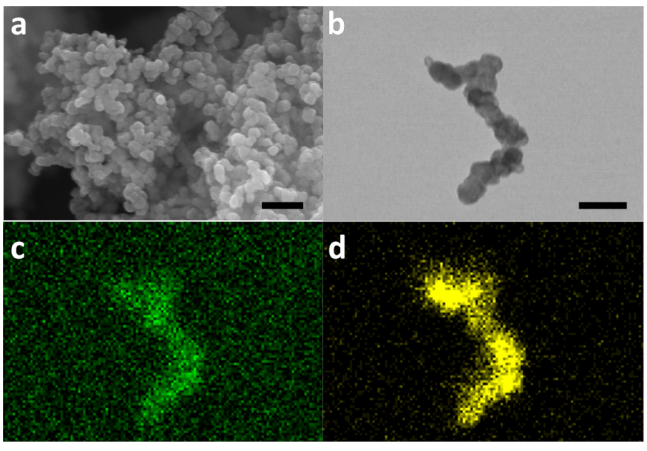

Figure 2. (a) SEM and (b) STEM images. The corresponding elemental maps show (d) a homogeneous sulfur distribution in (c) the carbon framework. Scale bar: 200 nm for both a and b. Note: a typical TEM grid coated with a carbon film was used, accounting for the presence of the background carbon.

Graphene-wrapping of the KBC/S was achieved by self-assembly between the positively charged KBC/S and negatively charged graphene oxide (GO). The KBC/S was first functionalized with the cationic polyelectrolyte poly(DADMAC) to create positive charges on the surface. This step enables the KBC/S to be dispersed in water to form a suspension. When this is added to a dilute GO dispersion, the positively charged KBC/S is encapsulated by negatively charged GO due to electrostatic interactions. Hydrazine was then added as the reducing agent to convert the GO to graphene. It is important to note that the reduction effect strongly depends on the reaction temperature and not only reaction time. For example, it is reported that the sp^2 structure of partly reduced GO only forms above 60 °C in the presence of hydrazine, which leads to a leap in electric conductivity from 1×10^{-6} S cm^{-1} to 5 S cm^{-1}.[35] However, it is thought that the functional groups on GO play an important role in the immobilization of lithium polysulfide species.[21] Thus, a compromise between highly conductive graphene and partially reduced GO with oxygen-containing groups remaining in the structure is necessary. To examine the role of temperature in controlling reduction, a GO dispersion (without KBC/S) was treated with hydrazine for 60 min between 25 and 70 °C. As shown in Figure 3, the sample

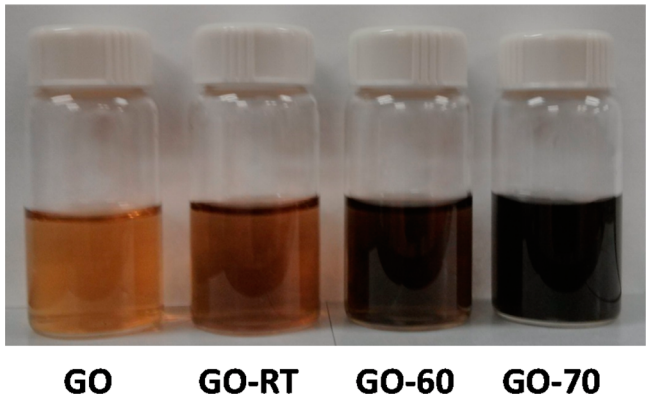

Figure 3. Images of a GO solution and the products reduced by hydrazine under various temperatures: room temperature (GO-RT), 60 °C (GO-60), and 70 °C (GO-70). GO and hydrazine concentrations are 0.1 mg mL^{-1} and 0.3 mg mL^{-1}, respectively. The reduction duration was 60 min for all three samples treated at different temperatures.

treated at room temperature (GO-RT) still appears brown in color, the sample treated at 60 °C (GO-60) is dark-brown, but the sample treated at 70 °C (GO-70) is essentially black. This result is consistent with the findings of previous studies that the C/O atomic ratio increases at elevated temperature because of the deep reduction of GO.[35] The optimal conditions are at 60 °C, where oxygen-containing functional groups on the GO-60 sample are still present, evidenced by characteristic bands in its FTIR spectrum owing to C−O (1410 cm^{-1}), C−O−C (1105 cm^{-1}), and C−OH (3450 cm^{-1}) species (Figure 4). At higher reduction temperatures (>70 °C), the product is mainly graphene[35] and sulfur dissolution from the KBC/S becomes problematic (see Figure S3 in the Supporting Information).

Figure 5 displays the electron microscope images of the encapsulated KBC/S composite at different magnifications. The

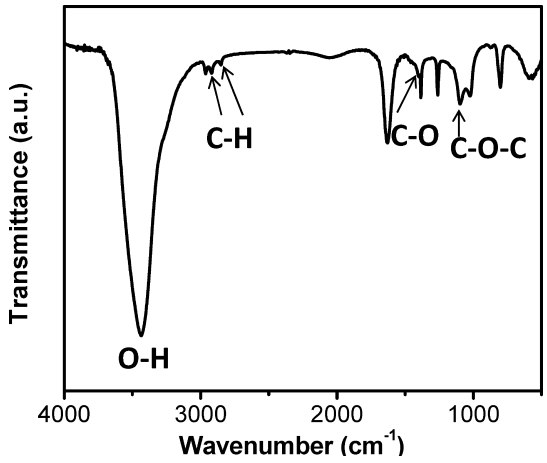

Figure 4. Fourier transform infrared spectroscopy (FTIR) of the GO treated at 60 °C with hydrazine; characteristic bands of oxygen-containing functional groups are indicated.

STEM and TEM images clearly show the graphene wrapping around the KBC/S composite (Figure 5a, b).

The low-magnification SEM image also shows the presence of looser encapsulation of the aggregated KBC/S nanoparticles (Figure 5c), which is likely due to the precipitation of an excess of reduced-GO sheets on the closely wrapped KBC/S composites. This unique close-loose graphene-wrapping of the mesoporous C/S nanostructure is different from most of the previously reported graphene cathodes.

The g-KBC/S material was evaluated as a sulfur cathode in coin cells with metallic lithium as the anode and 1 M LiTFSI in DOL+DME as the electrolyte between 2.7−1.8 V. The capacity−voltage profiles for different cycles of the Li−S cell at a current density of 168 mA g^{-1} ($C/10$) are presented in Figure 6a. The first discharge of the cell (black curve) displays a typical two-plateau process where the high plateau at 2.3−2.35 V is associated with each sulfur atom gaining about half an electron to form S_n^{2-} ($4 < n < 8$) polysulfide species. Further discharge reduces the S_n^{2-} ($4 < n < 8$) intermediates to S_2^{2-} and/or S^{2-} at the lower plateau (2.1 V). The charge process also consists of two plateaus at 2.25 and 2.4 V, respectively, indicating the two stage oxidation of Li_2S and/or Li_2S_2. The g-KBC/S cathode exhibits a capacity fading to 770 mAh g^{-1} within the first 15 cycles, and extremely stable cycling over the following cycles (Figure 6b). The discharge capacity on the 200th cycle is 740 mAh g^{-1}, which is 96.1% of the capacity of the 15th cycle (~770 mAh g^{-1}). The capacity loss over these 185 cycles is only 0.026% or 0.167 mAh g^{-1} per cycle, with a relatively high Coloumbic efficiency of ~98%. The stable cycling performance of the cell is coincident with the charge−discharge curves shown in Figure 6a. They are almost identical— except for some small capacity variation—from the 10th cycle onward.

The exceptionally good cyclability of the cathode is attributed to the unique configuration of the g-KBC/S. First, KBC is an ideal framework for sulfur: it has sufficiently small mesopores and large micropores to provide sufficient containment for 70 wt % sulfur, and additional textural porosity to accommodate for expansion on forming the lowest density sulfide, Li_2S. The nanoscale particle size of the carbon facilitates homogeneous sulfur distribution in the meso/micropores, one of the key factors to enable all of the sulfur to be reduced at the same rate. However, sulfur/polysulfide dissolution and the

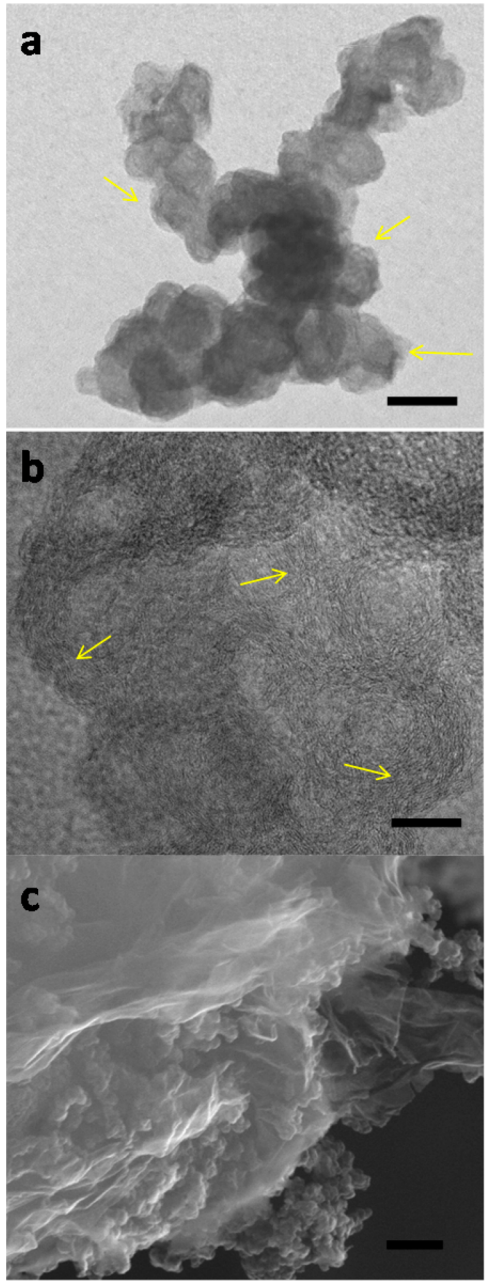

Figure 5. (a) STEM, (b) TEM and (c) SEM images of g-KBC/S showing the graphene-wrapping of KBC/S particles at various magnifications. Arrows in a and b indicate multilayer-graphene sheets on the surface of the C/S nanoparticles. Scale bar: 50, 20, and 200 nm for a, b, and c, respectively.

polysulfide shuttle cannot be avoided by simply employing a porous carbon as a framework. This is because the open porous structure provides paths for solvated polysulfide species in addition to solvated Li ions. Additionally, the hydrophobic carbon environment does not support interaction with polysulfides owing to their hydrophilic nature. Cycling stability can be greatly enhanced by either decorating the carbon with a hydrophilic polymer such as poly(ethylene glycol),[9] adding hydrophilic compounds[36,37] into the cathodes, or employing a less hydrophobic framework such as a conductive polymer[38] or TiO_2.[39] Once the polysulfides diffuse out from the nanopores into the electrolyte, they are more likely to precipitate as Li_2S on the exterior surface of the carbon framework on the

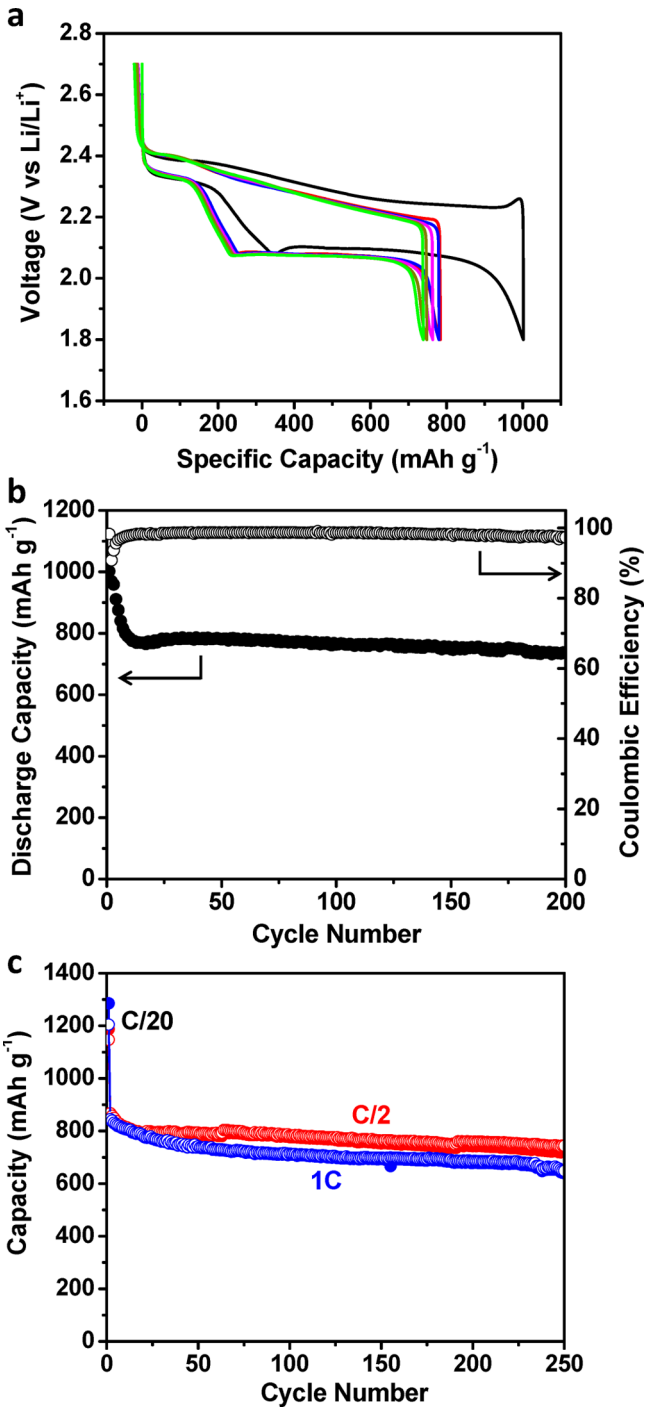

Figure 6. (a) Voltage−capacity profiles (black, 1st cycle; red, 10th cycle; blue, 50th cycle; magenta, 100th cycle; dark yellow, 150th cycle; and green, 200th cycle), and cycling performance at (b) *C*/10 and (c) *C*/2 and 1*C* (solid spheres, discharge capacity; hollow spheres, charge capacity) of the g-KBC/S cathodes.

subsequent reduction cycle.[40,41] Consequently, if the layer becomes sufficiently thick, electrical contact and ion transport is lost, gradually impairing cycling. This assumption is verified by using bare KBC/S as an electrode, where severe capacity fading is detected over 100 cycles under exactly the same charge−discharge conditions as for the g-KBC/S sample (see Figure S4 in the Supporting Information). The oxygen-containing groups on the graphene sheets provide a physical diffusion barrier, limit surface reduction (because of their poor conductivity), and contribute to the immobilization of the polysulfides in the cathode by modifying the hydrophobicity[42] and enhancing their binding.[20] Finally, the selected narrow electrochemical window (1.8−2.7 V) is another capacity retention optimization strategy. The electrolyte additive $LiNO_3$ participates in the reaction in the cathode below 1.7 V.[43] Some groups (including ours) have observed a third plateau in this range on the discharge curve and large irreversible capacities for the first few cycles.[44,45] Zhang et al. suggest use of $LiNO_3$ as a regular electrolyte salt instead of an additive as it is continuously consumed upon cycling.[46] By ending the discharge process at 1.8 V, both the third plateau and irreversible capacity are avoided (Figure 6a).

The cycling performance of the KBC/S cathodes was also studied at more practical rates, *C*/2 and 1*C*. Beforehand, the cells were discharged at a much slower rate (*C*/20) in order to condition the electrode and enable complete electrolyte wetting. The initial discharge capacities of the cells at *C*/2 and 1*C* are 863 and 843 mAh g^{-1}, respectively. Similar to the data collected at *C*/10, some capacity fade is observed on the first several cycles, but this is followed by very stable cycling (Figure 6c). After 250 cycles, capacity retention of 83.4% (720 mAh g^{-1}) and 75.9% (640 mAh g^{-1}) is achieved for *C*/2 and 1*C*, respectively, which suggests that the polysulfide shuttle is significantly suppressed at high rates as well.

CONCLUSIONS

In summary, we have demonstrated a strategy to prepare a graphene-encapsulated KBC/S nanocomposite via self-assembly between surfactant stabilized KBC/S nanoparticles and dispersed GO. Control of the reaction temperature and duration results in partial reduction of the GO, whereby a significant fraction of oxygen-containing groups are retained. The resulting sulfur cathode exhibits high reversible capacity over a long period, with average capacity fading of only 0.026% or 1.167 mAh g^{-1} per cycle over 185 cycles. To the best of our knowledge, this represents one of the best results for carbonaceous-based sulfur cathodes. This particularly stable cycling performance arises from the combined effects of mesoporous carbon and graphene, which successfully confine polysulfide species within the cathode. In addition, the oxygen-containing functional groups on the graphene sheets and the selected narrow electrochemical window are expected to be beneficial for polysulfide retention.

ASSOCIATED CONTENT

Supporting Information

SEM image and cumulative pore volumes of Ketjen black carbon and Ketjen black carbon/sulfur composites; TGA results of the KBC/S and g-KBC/S prepared at 60 and 70 °C; cycling performance of the Ketjen black carbon/sulfur cathode at *C*/2. This material is available free of charge via the Internet at http://pubs.acs.org.

AUTHOR INFORMATION

Corresponding Author

*E-mail: lfnazar@uwaterloo.ca.

Author Contributions

The manuscript was written through contributions of all authors. All authors have given approval to the final version of the manuscript.

Notes

The authors declare no competing financial interest.

■ ACKNOWLEDGMENTS

This research was supported by the BASF International Scientific Network for Electrochemistry and Batteries. We thank NSERC for generous support via a Canada Research Chair to LFN. We gratefully acknowledge N. Coombs, University of Toronto, for help with acquisition of the TEM images.

■ REFERENCES

(1) Bruce, P. G.; Freunberger, S. A.; Hardwick, L. J.; Tarascon, J.-M. Li-O_2 and Li-S batteries with High Energy Storage. *Nat. Mater.* **2012**, *11*, 19−29.
(2) Ji, X.; Nazar, L. F. Advances in Li-S Batteries. *J. Mater. Chem.* **2010**, *20*, 9821−9826.
(3) Yang, Y.; Zheng, G. Y.; Cui, Y. Nanostructured Sulfur Cathodes. *Chem. Soc. Rev.* **2013**, *42*, 3018−3032.
(4) Song, M.-K.; Cairns, E. J.; Zhang, Y. Lithium/Sulfur Batteries with High Specific Energy: Old Challenges and New Opportunities. *Nanoscale* **2013**, *5*, 2186−2204.
(5) Wang, D. W.; Zeng, Q.; Zhou, G.; Yin, L.; Li, F.; Cheng, H.-M.; Gentle, I. R.; Lu, G. Q. M. Carbon-Sulfur Composites for Li-S Batteries: Status and Prospects. *J. Mater. Chem. A* **2013**, *1*, 9382−9394.
(6) Evers, S.; Nazar, L. F. New Approaches for High Energy Density Lithium-Sulfur Battery Cathodes. *Acc. Chem. Res.* **2013**, *46*, 1135−1143.
(7) Barghamadi, M.; Kapoor, A.; Wen, C. A Review of Li-S Batteries as a High Efficiency Rechargeable Lithium Battery. *J. Electrochem. Soc.* **2013**, *160*, A1256−A1263.
(8) Mikkhaylike, Y. V.; Akridge, J. R. Polysulfide Shuttle Study in the Li/S Battery System. *J. Electrochem. Soc.* **2004**, *151*, A1969−A1976.
(9) Ji, X.; Lee, K. T.; Nazar, L. F. A Highly Ordered Nanostructured Carbon-Sulphur Cathode for Lithium-Sulphur Batteries. *Nat. Mater.* **2009**, *8*, 500−506.
(10) He, G.; Ji, X.; Nazar, L. F. High "C" Rate Li-S Cathodes: Sulfur Imbibed Bimodal Porous Carbons. *Energy Environ. Sci.* **2011**, *4*, 2878−2883.
(11) Schuster, J.; He, G.; Mandlmeier, B.; Yim, T.; Lee, K. T.; Bein, T.; Nazar, L. F. Spherical Ordered Mesoporous Carbon Nanoparticles with High Porosity for Lithium-Sulfur Batteries. *Angew. Chem., Int. Ed.* **2012**, *51*, 3591−3595.
(12) Zhang, B.; Qin, X.; Li, G. R.; Gao, X. P. Enhancement of Long Stability of Sulfur Cathode by Encapsulating Sulfur into Micropores of Carbon Spheres. *Energy Environ. Sci.* **2010**, *3*, 1531−1537.
(13) Liang, C.; Dudney, N. J.; Howe, J. Y. Hierarchically Structured Sulfur/Carbon Nanocomposite Material for High-Energy Lithium Battery. *Chem. Mater.* **2009**, *21*, 4724−4730.
(14) Xin, S.; Gu, L.; Zhao, N.-H.; Yin, Y.-X.; Zhou, L.-J.; Guo, Y.-G.; Wan, L.-J. Smaller Sulfur Molecules Promise Better Lithium-Sulfur Batteries. *J. Am. Chem. Soc.* **2012**, *134*, 18510−18513.
(15) Kim, J.; Lee, D.-J.; Jung, H.-G.; Sun, Y.-K.; Hassoun, J.; Scrosati, B. An Advanced Lithium-Sulfur Battery. *Adv. Funct. Mater.* **2012**, *23*, 1076−1080.
(16) Tachikawa, N.; Yamauchi, K.; Takashima, E.; Park, J.-W.; Dokko, K.; Watanabe, M. Reversibility of Electrochemical Reaction of Sulfur Supported on Inverse Opal Carbon in Glyme-Li Salt Molten Complex Electrolytes. *Chem. Commun.* **2011**, *47*, 8173−8159.
(17) Gao, J.; Lowe, M. A.; Kiya, Y.; Abruña, H. D. Effects of Liquid Electrolytes on the Charge-Discharge Performance of Rechargeable Lithium/Sulfur Batteries: Electrochemical and in-Situ X-ray Absorption Spectroscopic Studies. *J. Phys. Chem. C* **2011**, *115*, 25132−25137.
(18) Yim, T.; Park, M.-S.; Yu, J.-S.; Kim, K. J.; Im, K. Y.; Kim, J.-H.; Jeong, G.; Jo, Y. N.; Woo, S.-G.; Kang, K. S.; Lee, I.; Kim, Y.-J. Effect of Chemical Reactivity of Polysulfide Toward Carbonate-Based Electrolyte on the Electrochemical Performance of Li-S batteries. *Electrochim. Acta* **2013**, *107*, 454−460.
(19) Lu, S.; Cheng, Y.; Wu, X.; Liu, J. Significantly Improved Long-Cycle Stability in High-Rate Li-S Batteries Enabled by Coaxial Graphene Wrapping Over Sulfur-Coated Carbon Nanofibers. *Nano Lett.* **2013**, *13*, 2485−2489.
(20) Wang, L.; Wang, D.; Zhang, F.; Jin, J. Interface Chemistry Guided Long-Cycle-Life Li-S Battery. *Nano Lett.* **2013**, *13*, 4206−4211.
(21) Li, L.; Rao, M.; Zheng, H.; Zhang, L.; Li, Y.; Duan, W.; Guo, J.; Cairns, E. J.; Zhang, Y. Graphene Oxide as a Sulfur Immobilizer in High Performance Lithium/Sulfur Cells. *J. Am. Chem. Soc.* **2011**, *133*, 18522−18525.
(22) Wang, H.; Yang, Y.; Liang, Y.; Robinson, J. T.; Li, Y.; Jackson, A.; Cui, Y.; Dai, H. Graphene-Wrapped Sulfur Particles as a Rechargeable Lithium-Sulfur Battery Cathode Material with High Capacity and Cycling Stability. *Nano Lett.* **2011**, *11*, 2644−2647.
(23) Evers, S.; Nazar, L. F. Graphene-Enveloped Sulfur in a One Pot Reaction: a Cathode with Good Coulombic Efficiency and High Practical Sulfur Content. *Chem. Commun.* **2012**, *48*, 1233−1235.
(24) Li, N.; Zheng, M.; Lu, H.; Hu, Z.; Shen, C.; Chang, X.; Ji, G.; Cao, J.; Shi, Y. High-Rate Lithium-Sulfur Batteries Promoted by Reduced Graphene Oxide Coating. *Chem. Commun.* **2012**, *48*, 4106−4108.
(25) Zhang, F.-F.; Zhang, X.-B.; Dong, Y.-H.; Wang, L.-M. Facile and Effective Synthesis of Reduced Graphene Oxide Encapsulated Sulfur *via* Oil/Water System for High Performance Lithium Sulfur Cells. *J. Mater. Chem.* **2012**, *22*, 11452−11454.
(26) Park, M.-S.; Yu, J.-S.; Kim, K. J.; Jeong, G.; Kim, J.-H.; Jo, Y.-N.; Hwang, U.; Kang, S.; Woo, T.; Kim, Y.-J. One-Step Synthesis of a Sulfur-Impregnated Graphene Cathode for Lithium-Sulfur Batteries. *Phys. Chem. Chem. Phys.* **2012**, *14*, 6796−6804.
(27) Zhou, W.; Chen, H.; Yu, Y.; Wang, D.; Cui, Z.; DiSalvo, F. J.; Abruña, H. D. Amylopectin Wrapped Graphene Oxide/Sulfur for Improved Cyclability of Lithium-Sulfur Battery. *ACS Nano* **2013**, *7*, 8801−8808.
(28) Zhao, M.-Q.; Liu, X.-F.; Zhang, Q.; Tian, G.-L.; Huang, J.-Q.; Zhu, W.; Wei, F. Graphene/Single-Walled Carbon Nanotube Hybrids: One-Step Catalytic Growth and Applications for High-Rate Li-S Batteries. *ACS Nano* **2012**, *6*, 10759−10769.
(29) Cheng, Y.; Lu, S.; Zhang, H.; Varanasi, C. V.; Liu, J. Synergistic Effects from Graphene and Carbon Nanotubes Enable Flexible and Robust Electrodes for High-Performance Supercapacitors. *Nano Lett.* **2012**, *13*, 4206−4211.
(30) Chen, R.; Zhao, T.; Lu, J.; Wu, F.; Li, L.; Chen, J.; Tan, G.; Ye, Y.; Amine, K. Graphene-Based Three Dimensional Hierarchical Sandwich-Type Architecture for High-Performance Li/S Batteries. *Nano Lett.* **2013**, *13*, 4642−4649.
(31) Guo, C. X.; Li, C. M. A Self-Assembled Hierarchical Nanostructure Comprising Carbon Spheres and Graphene Nanosheets for Enhanced Supercapacitor Performance. *Energy Environ. Sci.* **2011**, *4*, 4504−4507.
(32) Yang, S.; Feng, X.; Ivanovici, S.; Müllen, K. Fabrication of Graphene-Encapsulated Oxide Nanoparticles: Towards High-Performance Anode Materials for Lithium Storage. *Angew. Chem., Int. Ed.* **2010**, *49*, 8408−8411.
(33) Jun, S.; Joo, S. H.; Ryoo, R.; Kruk, M.; Jaroniec, M.; Liu, Z.; Ohsuna, T.; Terasaki, O. Synthesis of New, Nanoporous Carbon with Hexagonally Ordered Mesostructure. *J. Am. Chem. Soc.* **2000**, *122*, 10712−10713.
(34) Meng, Y.; Gu, D.; Zhang, F.; Shi, Y.; Yang, H.; Li, Z.; Yu, C.; Tu, B.; Zhao, D. Ordered Mesoporous Polymers and Homologous Carbon Frameworks: Amphiphilic Surfactant Templating and Direct Transformation. *Angew. Chem., Int. Ed.* **2005**, *44*, 7053−7059.
(35) Ren, P.-G.; Yan, D. X.; Ji, X.; Chen, T.; Li, Z. M. Temperature Dependence of Graphene Oxide Reduced by Hydrazine Hydrate. *Nanotechnology* **2011**, *22*, 055705/1−055705/8.
(36) Ji, X.; Evers, S.; Black, R.; Nazar, L. F. Stabilizing Lithium-Sulphur Cathodes Using Polysulphide Reservoirs. *Nat. Commun.* **2011**, *2*, 325−331.
(37) Evers, S.; Yim, T.; Nazar, L. F. Understanding the Nature of Absorption/Adsorption in Nanoporous Polysulfide Sorbents for the Li-S Battery. *J. Phys. Chem. C* **2012**, *116*, 19653−19658.

(38) Seh, Z. W.; Li, W.; Cha, J. J.; Zheng, G.; Yang, Y.; McDowell, M. T.; Hsu, P.-C.; Cui, Y. Sulphur-TiO_2 Yolk-Shell Nanoarchitecture with Internal Void Space for Long-Cycle Lithium-Sulphur Batteries. *Nat. Commun.* **2013**, *4*, 1331 DOI: 10.1038/ncomms2327.
(39) Li, W.; Zheng, G.; Yang, Y.; Seh, Z. W.; Liu, N.; Cui, Y. High-Performance Hollow Sulfur Nanostructured Battery Cathode Through a Scalable, Room Temperature, One-Step, Bottom-Up Approach. *Proc. Natl. Acad. Sci. U.S.A.* **2013**, DOI: 10.1073/pnas.1220992110.
(40) Cheon, S.-E.; Ko, K.-S.; Cho, J.-H.; Kim, S.-W.; Chin, E.-Y.; Kim, H.-T. Rechargeable Lithium Sulfur Battery II. Rate Capability and Cycle Characteristics. *J. Electrochem. Soc.* **2003**, *150*, A800−A805.
(41) Nelson, J.; Misra, S.; Yang, Y.; Jackson, A.; Liu, Y.; Wang, H.; Dai, H.; Andrews, J. C.; Cui, Y.; Toney, M. F. In Operando X-ray Diffraction and Transmission X-ray Microscopy of Lithium Sulfur Batteries. *J. Am. Chem. Soc.* **2012**, *134*, 6337−6343.
(42) Zheng, G.; Zhang, Q.; Cha, J. J.; Yang, Y.; Li, W.; Seh, Z. W.; Cui, Yi. Amphiphilic Surface Modifications of Hollow Carbon Nanofibers for Improved Cycle Life of Lithium Sulfur Batteries. *Nano Lett.* **2013**, *13*, 1265−1270.
(43) Zhang, S. S. Liquid Electrolyte Lithium/Sulfur Battery: Fundamental Chemistry, Problems, and Solutions. *J. Power Sources* **2013**, *231*, 153−162.
(44) He, G.; Evers, S.; Liang, X.; Cuisinier, M.; Garsuch, A.; Nazar, L. F. Tailoring Porosity in Carbon Nanospheres for Lithium-Sulfur Battery Cathodes. *ACS Nano* **2013**, *7*, 10920−10930.
(45) Su, Y.-S.; Fu, Y.; Manthiram, A. Self-Weaving Sulfur-Carbon Composite Cathodes for High Rate Lithium-Sulfur Batteries. *Phys. Chem. Chem. Phys.* **2012**, *14*, 14495−14499.
(46) Zhang, S. S. Role of $LiNO_3$ in Rechargeable Lithium/Sulfur Battery. *Electrochim. Acta* **2012**, *70*, 344−348.